Supplementary information

Catalytic effect of silver plasmonic nanoparticles on the redox reaction leading to the $ABTS^{\bullet+}$ formation studied by UV-visible and Raman spectroscopy

A. Garcia-Leis[1], D. Jancura[2,3], M. Antalik[4,5], J.V. Garcia-Ramos[1], S. Sanchez-Cortes[1] and Z. Jurasekova[2,3*]

[1]*Instituto de Estructura de la Materia, IEM-CSIC, Serrano 121, 28006 Madrid, Spain*

[2]*Department of Biophysics, Faculty of Science, P.J. Safarik University in Kosice, Jesenna 5, 041 54 Kosice, Slovak Republic*

[3]*Center for Interdisciplinary Biosciences, Faculty of Science, P.J. Safarik University in Kosice, Jesenna 5, 041 54 Kosice, Slovak Republic*

[4]*Institute of Experimental Physics, SAS, Watsonova 47, 041 01 Kosice, Slovak Republic*

[5]*Department of Biochemistry, Faculty of Science, P.J. Safarik University in Kosice, Srobarova 2, 040 01 Kosice, Slovak Republic*

Figure S1. UV-visible absorption spectrum of 5 x 10^{-6} M ABTS aqueous solution. ***Inset:*** Chemical structure of the ABTS molecule.

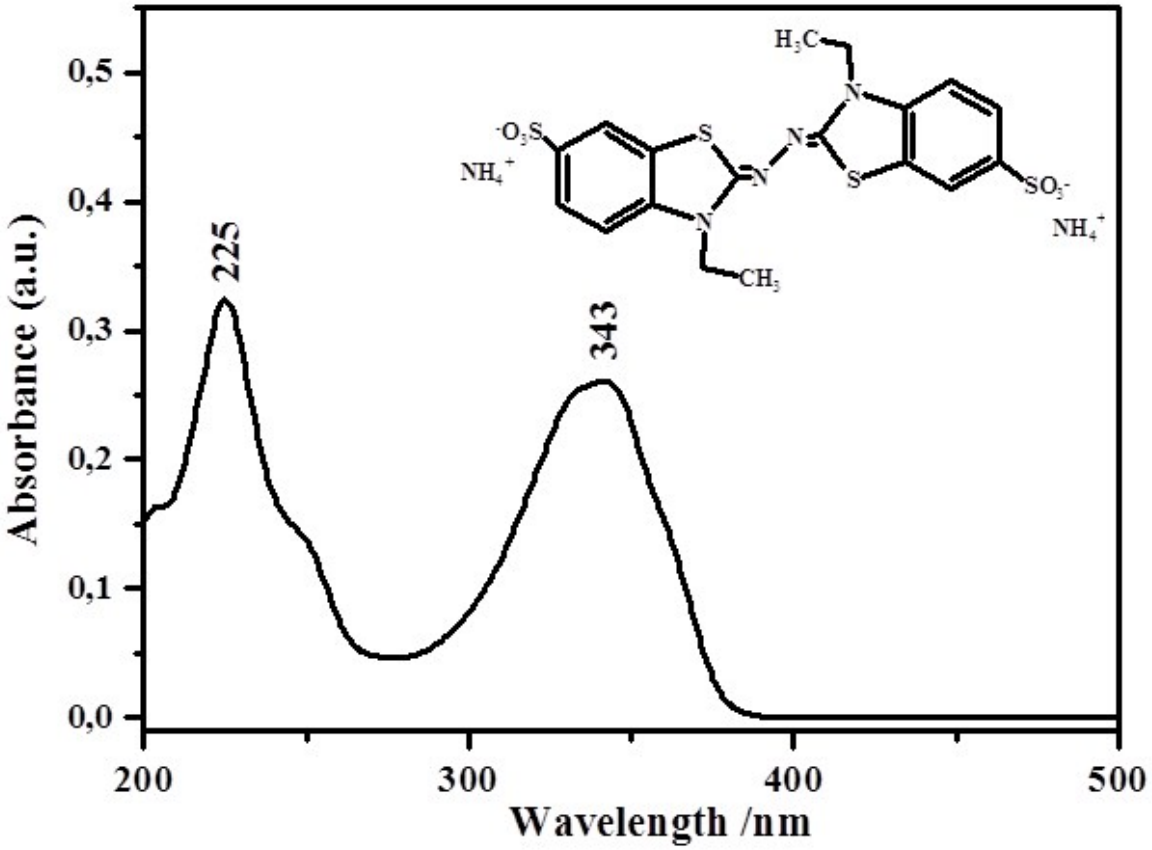

Figure S2. Time-dependent plots of the obtained intensity variations corresponding to the absorption maxima of the ABTS species observed at ~ 340 nm (**black**) and $ABTS^{\bullet+}$ at 415 and 730 nm (**red**) in the presence of AgH NPs **(A)** and AgNS NPs **(B)** at pH 2.5. AgH colloids with plasmon at 400, 403, 409 and 411 nm; and AgNS colloids having plasmon at 378, 378, 379 and 381 nm, were used.

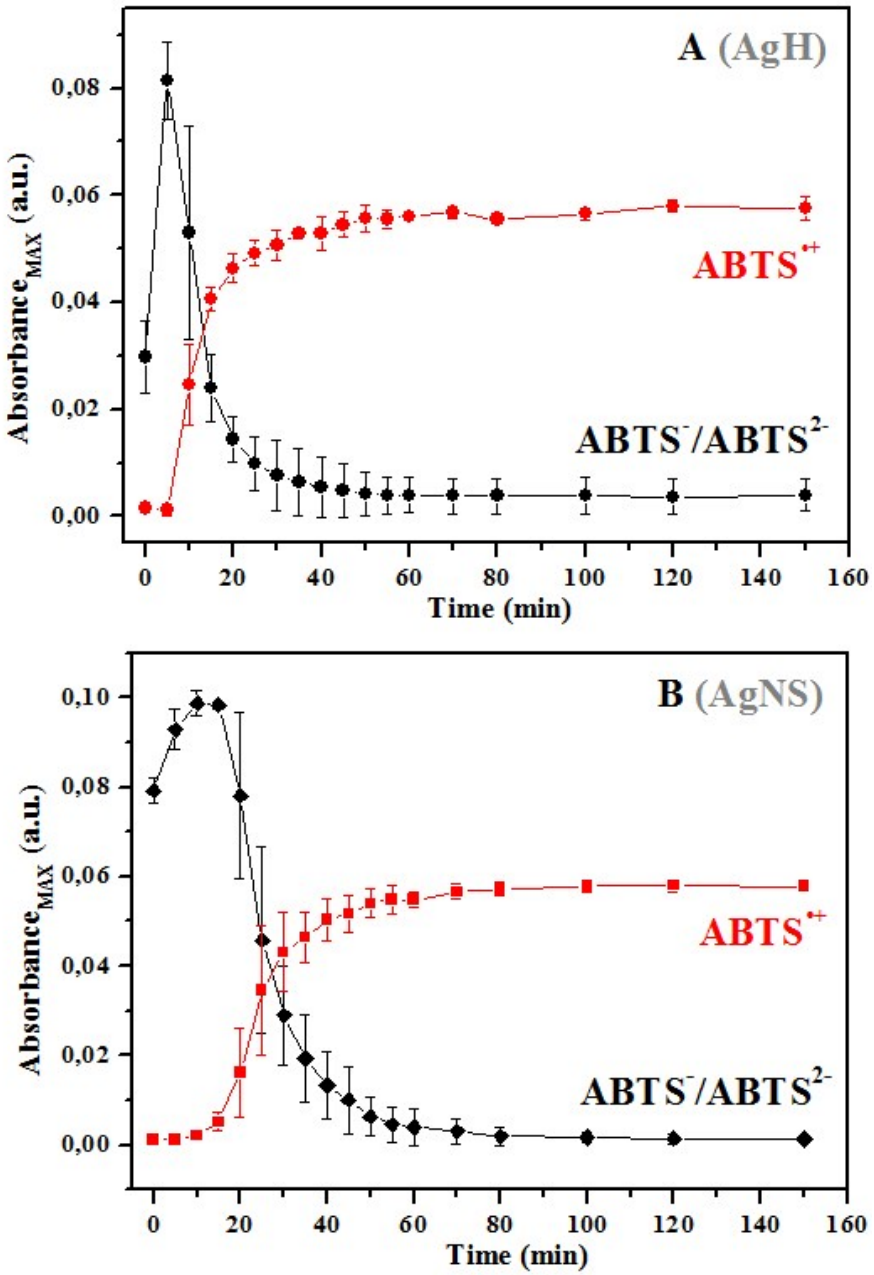

Table S1. Most probable band assignment of the ABTS Raman spectrum in the solid form and aqueous solution at pH=2.5 and at pH=1.5 (≈ subtracted spectrum: Raman spectrum recorded at pH=1.5 – Raman spectrum recorded at pH=2.5); and in concentrated HNO_3. All the spectra have been recorded using excitation at 532 nm.

Observed wavenumbers /cm^{-1}				**Assignment [b] (description)**
solid [a] ***Fig. 4a***	**solution; pH=2.5 [a]** ***Fig. 4d***	**solution; pH=1.5 - pH=2.5 [a]** ***Fig. 4g***	**solution; in HNO_3 [a]** ***Fig. 4f***	
1603 *vs*	1600 *vs*	1589 *m*	1590 *w*	$\nu(C=C)_{BM}$; $\nu_{as}(S\text{-}C=N)$
1578 *m, sh*	1577 *m, sh*	1574 w, *sh*	1567 *vw, sh*	$\nu(C=C)_{BM}$; $\nu_{s}(N\text{-}C=N)$
1485 *w*	1482 *w*	1482 *m*	1494 *w, sh*	$\delta(CH_3)$; $\nu(CC)_{BM}$
1466 *vw, sh*	1465 *vw, sh*		1464 *m*	$\delta(CH_3)$; $\delta(CH_2)$
		1454 *m, sh*		
		1441 *s*		$\gamma(CH_3)$; $\nu(CH_3)$; $\nu(CC)_{BM}$
1418 *vw*	1419 *vw*			$\delta(CH_2)$; $\delta(CH)_{BM}$; $\delta(NCH_3)$
		1402 *vs*	1416 *s*	$\nu(N=N)$
1389 *vw, sh*			1390 *w/m, sh*	$\gamma(CH_3)$; $\delta(CH)_{BM}$;
1379 *vw*	1380 *w/m*	1375 m		$\nu_{as}(NCC)$
1356 *w*	1360 *w*			$\nu(CC)$; $\nu_{as}(NCH_3)$; $\nu(CS)$;
		1340 w, *sh*	1348 *s*	$\delta(CH_3)$
1335 *vw*	1335 *vw*			$\nu(CC)$; $\nu_{s}(NCH_3)$
1310 *vw*	1310 *w*	1318 *m*	1324 *w/m, sh*	$\delta(CH)$; $\nu(CC)$; $\delta(CH3)$
1274 *vw*	1276 *vw*	1276 *w/m*	1276 *w*	$\nu_{as}(SO_2)$
1249 *vw*	1248 *w*	1252 *w/m*		$\nu_{s}(SO_2)$; $\nu(CN)_{TM}$
			1226 *vs*	$\nu(CH)$
		1202 *m*	1165 *w*	$\nu_{as}(SO_3\text{-}H)$
1144 *m*	1151 *m*	1153 *w/m*		$\rho(CH_2)$; $\rho(CH_3)$; $\nu(CC)_{alif}$

1130 *vw, sh*	1130 *vw, sh*	1132 *w/m*	1115 *m/s* 1090 *w/m*	δ(CH)
1098 *w*	1096 *w*	1095 *w*	1075 *w, sh*	$\nu_s(SO_3\text{-}H)$
1078 *w*	1075 *w*	1067 *w, sh*	1054 *w*	ρ(CH3); δ(CH); ν(CSC)
1052 *w/m*		1048 *s*	1029 *w*	$\delta(CH)_{BM}$
1041 *w/m*	1038 *m*		1004 *vw* 945 *vw*	$\rho(CH_2)$; $\rho(CH_3)$
938 *w*	936 *vw*	940 *vw*		$\rho(CH_3)$; $\delta(CH)_{BM}$
857 *w*	854 *w*	859 *w*		ν_{TM}; $\delta(CH)_{BM}$
		774 *w*		$\nu_{as}(CS)_{TM}$
749 *w*	751 *vw*	756 *vw*		$\nu_s(CS)_{TM}$; $\delta(CH)_{BM}$
		686 *w*	684 *vw*	$\gamma(CSC)_{TM}$
633 *vw*		627 *vw, br*		$\delta(NCS)_{TM}$

[a] *vw: very weak; w: weak; m: medium; s: strong; vs: very strong; sh: shoulder; br : broad*

[b] ν*: stretching;* δ*: in-plane bending;* γ*: out-of-plane bending;* ρ*: rocking; s: symmetric; as: antisymmetric; BM – benzene moiety; TM – thiazole moiety (Figure S1)*

Table S2. Characteristic (the most intense) wavenumbers observed in the Raman spectra of 10mM ABTS in concentrated HNO_3 and in aqueous solution at pH 1.5 (≈ subtracted spectrum: Raman spectrum recorded at pH=1.5 – Raman spectrum recorded at pH=2.5) corresponding to the Raman spectra of $ABTS^{2+}$ and $ABTS^{\bullet+}$, respectively; compared to the wavenumbers observed in the SERS spectra of ABTS obtained at pH 2.5 in time 0 minutes and 120 minutes after mixing of ABTS solution with AgH NPs; and by using AgNS at pH 2.5.

Observed wavenumbers /cm^{-1}				
Raman in HNO_3 *Fig. 4f*	**SERS (AgH) pH 2.5, time: 0 min** *Fig. 5d*	**SERS (AgH) pH 2.5, time: 120 min** *Fig. 5f*	**Raman solution; pH=1.5 - pH=2.5** *Fig. 4g*	**SERS (AgNS) pH 2.5** *Fig. 5b*
$ABTS^{2+}$		**$ABTS^{\bullet+}$**		
		1483	**1482**	**1483**
		1441	**1441**	**1442**
1416	**1409**			
		1403	**1402**	**1403**
		1376	**1375**	**1377**
1348	**1342**			
1324	**1318**			
1226	**1226**			
		1205	**1202**	**1205**
1115	**1113**			

Figure S3. Plot of the intensity of the ν(Ag-Cl) vibration band, visible at ~ 240 cm^{-1}, normalized to the 3400 cm^{-1} water band *vs.* time. All the spectra have been recorded using excitation at 532 nm. ***Inset:*** The selection of the spectral range showing the analyzed band registered in time 0 and 150 minutes after mixing of ABTS and AgH NPs solutions.

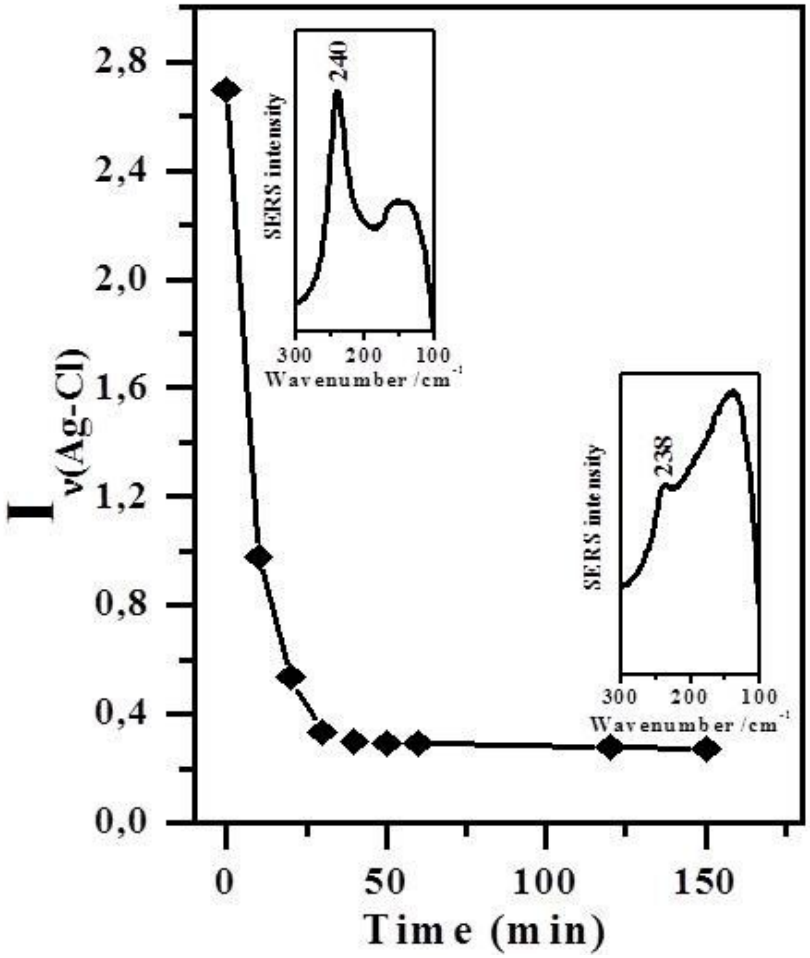

Figure S4. (A) Micrographs of AgNS and AgNS/ABTS system obtained by TEM at different times after mixing of ABTS and AgNS solutions. **(B)** TEM and SEM images of formed ABTS microcrystals covered with the small Ag clusters. The red arrowheads indicate some of the Ag clusters.

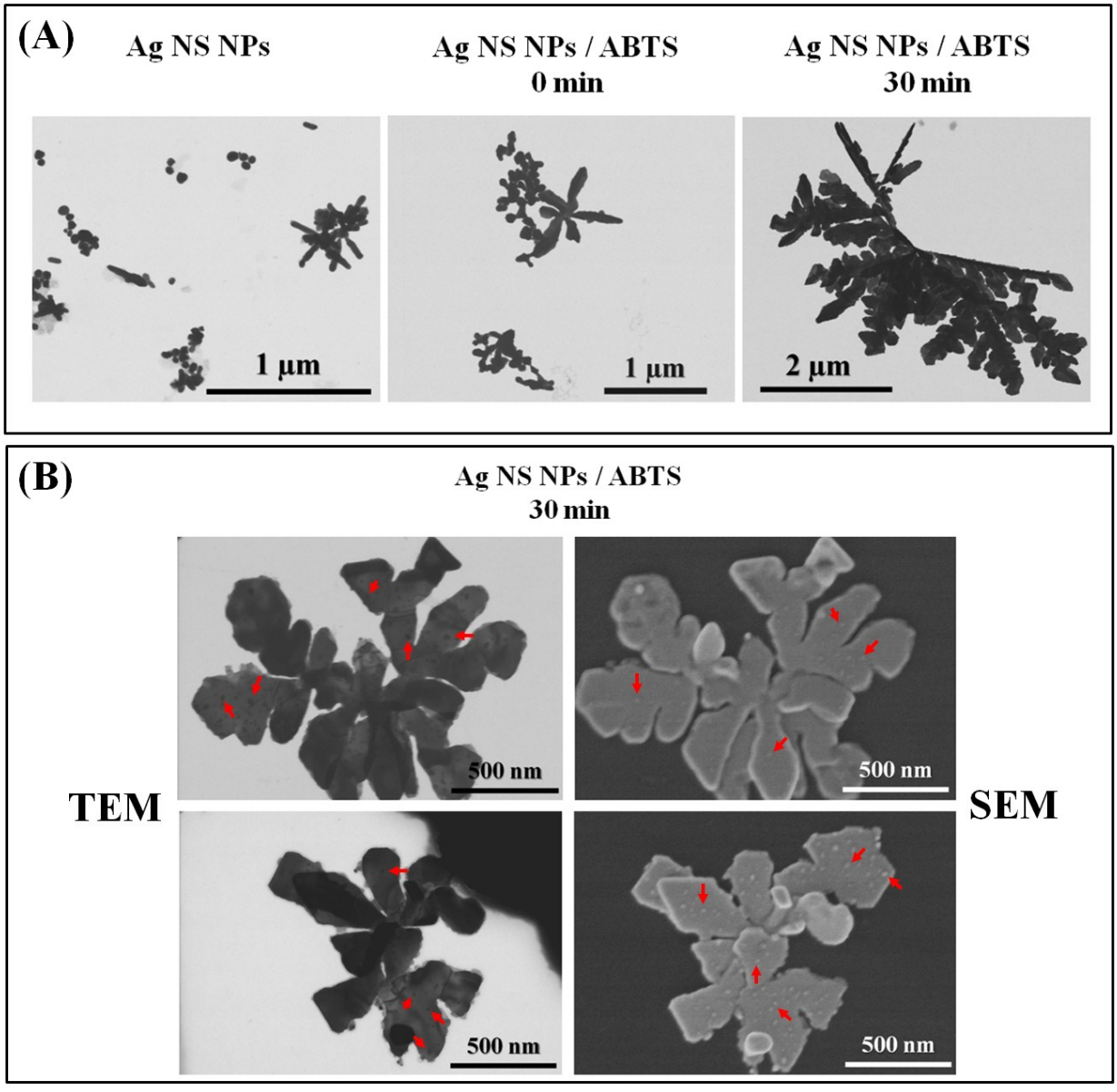

Figure S5. Adsorption isotherm obtained from the variation of the relative intensity of $ABTS^{\bullet+}$ bands at ~ 1400 cm^{-1} on AgNS NPs at different ABTS concentrations. ***Inset:*** Linear fitting at low molecule concentrations. All the spectra have been recorded using excitation at 532 nm.

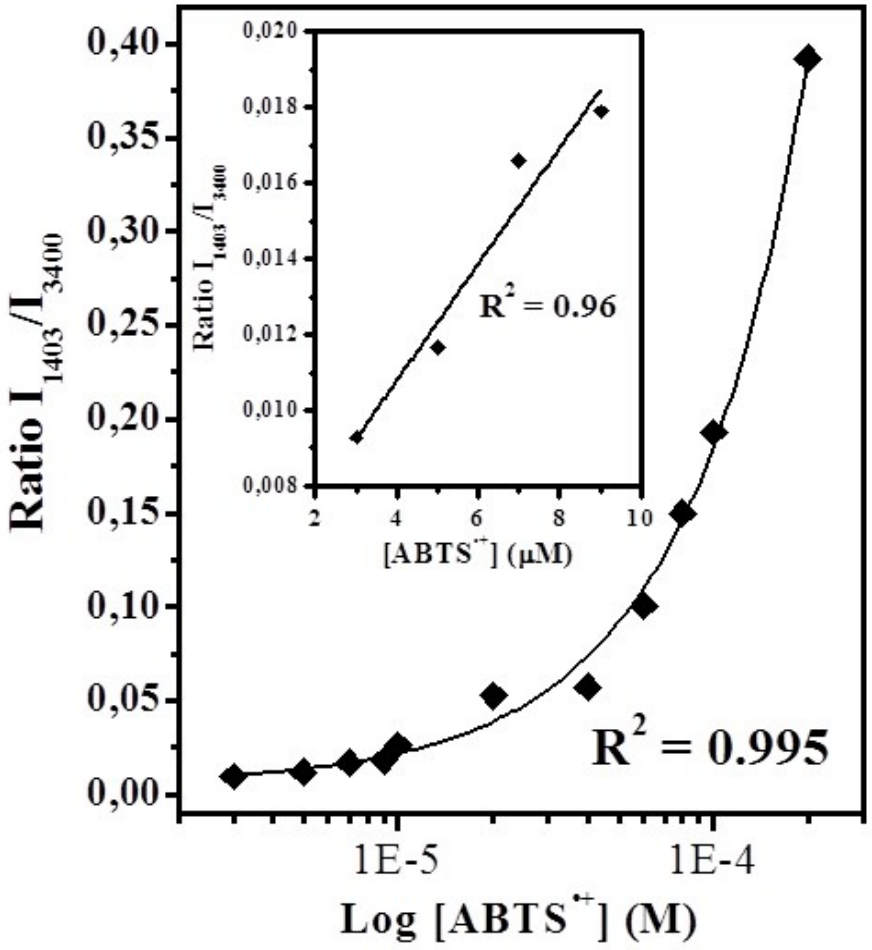

Determination of the limit of detection of the $ABTS^{\bullet+}$ for the ABTS/AgNS NPs system.

SERS spectra of the ABTS on AgNS NPs at various concentrations of ABTS were recorded in order to determine the parameters related to the adsorption and interaction of the ABTS with AgNS NPs. The marker band of $ABTS^{\bullet+}$ placed at ~ 1400 cm^{-1} was chosen to obtain the corresponding concentration curve since the position and the shape of the band did not change as the concentration of the ABTS molecule varies. The intensity of the 1400 cm^{-1} was normalized with the water band at 3400 cm^{-1}. We can then consider that [ABTS] ≅ [$ABTS^{\bullet+}$], since the original species (ABTS) is finally converted into the radical cation ($ABTS^{\bullet+}$) by the effect of the metal surface.

Figure S5 shows the concentration dependence of the normalized 1400 cm^{-1} marker band intensity of $ABTS^{\bullet+}$. The obtained adsorption isotherm follows an exponential variation far from the usual Langmuir adsorption model indicating that the final Raman spectrum does not fully correspond to the SERS effect caused by the formation of a monolayer of the molecules adsorbed on a plasmonic surface. On the contrary, the presence of cooperative effects derived from a possible intermolecular interaction and the corresponding conversion of ABTS in radical cation could lead to a different adsorption model. In addition, we are detecting characteristic Raman bands of $ABTS^{\bullet+}$ by [ABTS] variation what also indicates that even other energetic processes can contribute to the observed curve.

However, at low ABTS concentrations the exponential curve becomes linear and can be expressed in function of the radical cation concentration as follows:

$$I_{SERS} \cong K'[ABTS] \cong K[ABTS^{\bullet+}] \qquad \text{Eq. S1}$$

where we can consider that all the ABTS species are finally converted in the corresponding radical cation on the metal surface, and K is a constant that refers to all the possible effects taking place in the overall process (reduction, adsorption, etc.).

The limit of detection (LOD) can be deduced from the above linear dependence, as shown in the inset of Fig. S5, by considering the concentration $[ABTS^{\bullet+}]_{LOD}$, at which a relative intensity of 3σ is obtained, with σ being the standard deviation of the blank measurement:

$$3\sigma = A + B\,[ABTS^{\bullet+}]_{LOD} \qquad \text{Eq. S2}$$

$$[ABTS^{\bullet+}]_{LOD} = \frac{3\sigma - A}{B} \qquad \text{Eq. S3}$$

The LOD obtained in this work is $[ABTS^{\bullet+}]_{LOD} = 1.65 \times 10^{5} mol/L = 0.009056 g/L = 9.06\ ppm$.